



# Ecological aspects and hydrodynamics of hitchhiking remoras *Remora* spp. associated with sicklefin devil rays *Mobula tarapacana*

Gloria Castellano-González<sup>1,#</sup>, Bruno C. L. Macena<sup>1,2,#,\*</sup>, Tiago Bartolomeu<sup>3</sup>,  
André Passos<sup>3</sup>, Pedro Afonso<sup>1,2</sup>, Jorge Miguel Rodrigues Fontes<sup>1</sup>

<sup>1</sup>OKEANOS Institute of Marine Sciences, University of the Azores, Prof. Dr. Frederico Machado St., 4, 9901-862 Horta, Portugal

<sup>2</sup>Instituto do Mar (IMAR), Prof. Dr. Frederico Machado St., 4, 9901-862 Horta, Portugal

<sup>3</sup>Centre for Engineering and Product Development (CEiiA), D. Afonso Henriques Ave., 1825, 4450-017 Matosinhos, Portugal

**ABSTRACT:** Remoras are the most common symbiont of pelagic devil rays (Mobulidae). They attach to the host using a modified dorsal fin that acts as a suction cup, an adaptation to provide enhanced protection from predators and feeding opportunities, facilitate encounters with conspecifics and save energy by reducing the remora's cost of transport. Much less clear is whether mobulids obtain any benefits or even if this symbiosis impacts them. These ecological interactions have only been addressed for some species (e.g. sharks, cetaceans and turtles) but not yet for the sicklefin devil ray *Mobula tarapacana*. To understand the remora's attachment body site preferences, the hydrodynamic influence on the site selection and the drag cost of transport to the host, the remora–devil ray association was investigated in the Azores archipelago (Portugal) by combining *in situ* surveys with animal-borne video monitoring and 3-dimensional fluid modelling analyses. Our study identifies the common remora *Remora remora* as the main symbiont of adult sicklefin devil rays and describes the number of remoras per host, their size structure and preferred attachment position, plus the hydrodynamic cost to the devil rays. We found that individual sicklefin devil rays usually carry 2 to 3 remoras (including large to small remoras), and remoras choose to attach to the head and tail of the sicklefin devil rays, to benefit from minimised drag. Our results also highlight that the overall drag resulting from the transportation of remoras is a relatively low hydrodynamic burden to the sicklefin devil rays.

**KEY WORDS:** Symbiont ecology · Symbiont spatial distribution · Microhabitat · Parasitic drag · Host hydrodynamics

## 1. INTRODUCTION

Echeneidae, from the Greek *echein* (to hold) and *naus* (a ship), is a family of fishes colloquially recognised as remoras; in Latin, the name *remora* means delay/hindrance and arose from an ancient superstition (Günther 1860, Heemstra 1986). Remoras or suckerfishes are a group of marine fishes well known for compliantly clinging to a variety of hosts, including sharks and pelagic mobulid (devil and

manta) rays (O'Toole 2002, Brunnschweiler & Sazima 2008, Kenaley et al. 2019, Becerril-García et al. 2020, Nicholson-Jack et al. 2021). Remoras, comprising 3 genera (*Echeneis*, *Phtheichthys* and *Remora*) and 8 valid species (O'Toole 2002, Parenti 2021), can be identified morphologically by having a transversally laminated oval-shaped disc on the head, homologous with a spinous dorsal fin, which they use to attach to the host (Whitehead 1984, O'Toole 2002, Kenaley et al. 2019).

<sup>#</sup>These authors contributed equally

\*Corresponding author: [brunomacena@hotmail.com](mailto:brunomacena@hotmail.com)

© The authors 2025. Open Access under Creative Commons by Attribution Licence. Use, distribution and reproduction are unrestricted. Authors and original publication must be credited.

The life history of remoras in the wild is poorly known, especially in the early phases, albeit several attempts have been made to understand the evolutionary forces behind their unique behaviour. For instance, the sharksucker *Echeneis naucrates* begins the attaching (i.e. symbiotic) phase when they reach 55 mm standard length (SL) (Nakajima et al. 1987), upon which they have been documented to show a high urge to attach to hosts and to reattach to the same location on their original host following detachment (Strasburg 1962). This behaviour highlights a preference for certain attachment locations on the host, possibly because of the differing hydrodynamic costs associated with each location that may act as a force of selection (Strasburg 1962, Brunnschweiler et al. 2020). Despite attempts to better understand the physics of the attachment mechanisms (Gamel et al. 2019) and to quantify the primary force that remoras need to overcome (i.e. fluid drag) to maintain attachment (Fish et al. 2006, Beckert et al. 2015, Xu et al. 2021), information on spatial dynamics and the reason remoras seem to select specific positions on their host is still lacking (Silva & Sazima 2008, Amin et al. 2016, Flammang et al. 2020, Wingert et al. 2021).

The ectosymbiotic facultative relationship between remoras and mobulids is widely reported (O'Toole 2002, Becerril-García et al. 2020, Nicholson-Jack et al. 2021), although there is still a striking lack of evidence to understand the ecological nature of remora–host association (Gayford 2024). Interspecific interactions can either benefit or harm both species, or not affect either (Mathis & Bronstein 2020), and the tradeoffs defining these interactions are often context dependent (Brunnschweiler et al. 2020). Therefore, a deeper understanding of the net effect of this symbiosis is necessary to understand the ecological relationship of both species (Mathis & Bronstein 2020, Gayford 2024).

Hitchhiking remoras have been hypothesised to benefit from protection against predators, reduced costs of transport, increased access to conspecifics for mating, increased food availability and facilitated ventilation (Leung 2014, Gamel et al. 2019). Some studies documented remoras feeding on the parasitic copepods living on their hosts (Cressey & Lachner 1970, O'Toole 2002) and thus claimed that this relationship is beneficial for remoras and probably also for their hosts, as it would provide the host with cleaning services. However, this is contingent on a negligible drag from the attached remoras (Oliver et al. 2011, Leung 2014).

Sicklefin devil rays *Mobula tarapacana* are a highly migratory species, primarily oceanic but also observed

in coastal waters, distributed circumglobally in tropical, subtropical and temperate waters of the Pacific, Atlantic and Indian oceans and known to aggregate seasonally in a few spots globally (Couturier et al. 2012, Palacios et al. 2023) including small islands, shallow pinnacles and seamounts of the Atlantic Ocean (Sobral & Afonso 2014, Thorrold et al. 2014). They are one of the largest mobulid species, attaining a maximum size of 3700 mm disc width (DW) (White et al. 2018), capable of diving frequently to the mesopelagic zone and even reaching bathypelagic depths to nearly 2000 m, during which they can experience temperatures as cold as 5°C and swim as fast as 6 m s<sup>-1</sup> (Thorrold et al. 2014). These vertical movements must pose extreme challenges to the remoras, as the movement was hypothesised as an attempt by the devil ray to remove parasites, including the remoras (Braun et al. 2022). Yet, remoras were observed hitchhiking on sicklefin devil rays and whale sharks *Rhincodon typus* at least down to 1400 m depth and 3.6°C water temperature (Fontes et al. 2023), suggesting that some remoras accompany their hosts to bathypelagic depths and are resistant to the extreme conditions. It remains unclear whether such deep dives would impact remora behaviour or physiology, and information regarding the basic elements of the association is still lacking.

Taking advantage of the opportunity offered by these unique Azorean sicklefin devil ray aggregations, the present study combined *in situ* observations with animal-borne video monitoring and 3-dimensional (3D) fluid modelling techniques to describe the remora–sicklefin devil ray interaction in oceanic insular aggregations. Specifically, we investigated (1) if the remora's attachment site preferences are random on the host's body, (2) if the hydrodynamics of the host influence the site selection and (3) if the remora load (i.e. drag cost of transport) is detrimental for the sicklefin devil ray. Furthermore, aspects of the remora population structure, fidelity to the host and the ecological relevance of this interaction were also discussed.

## 2. MATERIALS AND METHODS

### 2.1. Study area

The Azores archipelago, Portugal, is a group of 9 isolated volcanic islands on the mid-north Atlantic ridge (33.5–43.0° N, 21.0–35.5° W). Shallow seabeds <600 m depth cover a mere 1% of the ca. 1 million km<sup>2</sup> of the Azorean exclusive economic zone (Morato et

al. 2008), mostly corresponding to the numerous seamounts and dynamic topographic features on the islands' slopes that characterise this region. This includes the shallow reefs of the Princess Alice Bank (PAL, 45 nautical miles [nmi] southwest of Faial Island) and Baixa do Ambrósio (AMB, 3 nmi northwest of Santa Maria Island), where sicklefin devil rays are known to aggregate in relatively large numbers during the summer (Thorrold et al. 2014).

## 2.2. Data collection

### 2.2.1. Surveys

Underwater surveys were conducted at PAL and AMB from July to October 2018 to 2021. During the boreal summer surveys, we used stereo-video camera systems (3D stereophotogrammetry) to measure body size and investigated the interaction between the sicklefin devil ray (host) and remoras (hitchhiker) (Fig. 1A) close to the surface at these 2 aggregation sites. Additional footage of these interactions provided by citizen scientists and staff from local diving operators and animal-borne footage (see Section 2.2.3) were also used. One video source per day of survey (i.e. footage from only 1 of the divers) covering depths from the surface to ca. 30 m was then used for subsequent data extraction. For each survey, sicklefin devil rays that could be individually identified by their natural marks (i.e. scars, remora suction marks or pigmentation patterns between the grey and white area in the ventral side) were selected for data extraction. Alternatively, only the frame containing the maximum number of individuals (MaxN) for each survey was used to extract data. This process was adopted to avoid pseudo-replication resulting from repeated observations of the same devil ray on a given day (Millar & Anderson 2004, Wingert et al. 2021). However, the non-repeated observation of devil ray individuals (i.e. same individual sampled on different days) cannot be guaranteed across all of the data sets.

Data collected from the videos relative to hitchhiking remoras included (1) the species identification using available guides (O'Toole 2002, Bray 2019, Froese & Pauly 2019, Flammang et al. 2020, Wingert et al. 2021), (2) their size relative to the host (see Section 2.2.2 for more details on the measurement), (3) pigmentation (i.e. albino or regular), (4) behaviour (i.e. swimming, hovering, attached or feeding) and (5) position on the host (including the suction injury marks). Information on the host included the total number and individual position of remoras on the

ventral and dorsal sides coupled with their behaviour (i.e. swimming, gliding or feeding). The presence or absence of remoras on the host was determined for a subset of 346 devil rays from 77 video frames (i.e. survey days) containing the MaxN.

### 2.2.2. Stereophotogrammetry

The stereo-video camera system consisted of a pair of GoPro Hero 4+™ cameras in their standard underwater housing, mounted 800 mm apart on a bar and converged 6° inwards (Shortis et al. 2009, Sequeira et al. 2016). The camera system was calibrated prior to each field season following the software's instructions (CAL stereo-camera calibration software, SeaGIS) (Shortis & Harvey 1998, Boutros et al. 2015), and the camera housing positions were maintained fixed relative to each other throughout the seasons. Next, the stereo-video files from both cameras were simultaneously analysed according to software specifications (EventMeasure v5.22, SeaGIS). Accuracy for each length measurement was estimated by RMS (in mm) values. According to the software developer (SeaGIS), measurements that generate RMS values <20 are considered to be accurate. Due to issues with the calibration, measurements from 2019 and 2020 showed RMS values greater than the manufacturer's recommended threshold of 20 mm. High RMS values do not significantly affect sizing accuracy across fish taxa (Letessier et al. 2013), and the mean SL for remoras when RMS values were >20 was not significantly different from the mean SL when RMS values were <20 (unpaired *t*-test,  $p < 0.2129$ ); nonetheless, these measurements were retained.

DW and disc length (DL) measurements (in mm) available for the same devil ray individual ( $n = 13$ ) were strongly correlated (simple linear regression of correlation of Pearson:  $DW = 1.348 \times DL + 420.7$ ;  $R^2 = 0.964$ ; *t*-test:  $df = 11$ ,  $p < 0.001$ ). This equation was applied to estimate DW for individuals in which DW could not be measured. A subsample of videos from stereophotogrammetry was also used to measure remora ( $n = 46$ ) SL (in mm) (Edwards 1990).

### 2.2.3. Animal-borne video camera

Animal-borne supplementary footage from individually tagged sicklefin devil rays was used to describe the association/behaviour of the remoras on the host when they were away from the survey area. Video files were automatically synchronised with depth,

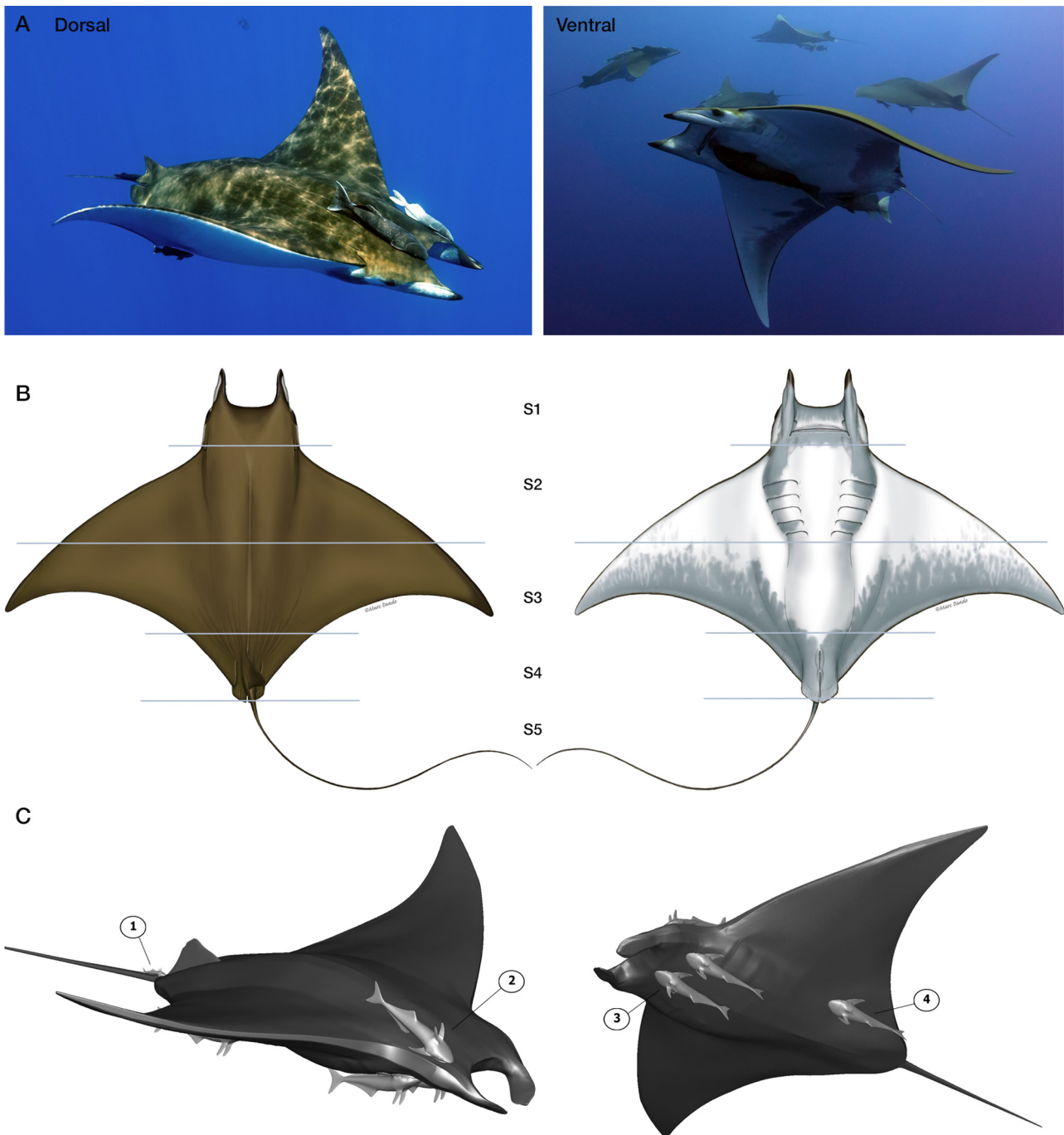


Fig. 1. (A) Dorsal (left) and ventral (right) underwater images of a sicklefin devil ray *Mobula tarapacana* at the Azorean aggregation sites showing the most common scenarios of remora association; (B) dorsal and ventral model images showing the 5 sectors (grey lines, S1–S5) used to describe the distribution and abundance of associated remoras (©Marc Dando, with permission); (C) the 4 location references for the hydrodynamic simulation model scenarios, 01, 02 and 03 for attached remoras and 04 for a remora hovering at the most common position (ventral side)

temperature and velocity by the tag's internal processor (for i-Pilot tag technical specifications of the camera and tagging procedure, see Fontes et al. [2022]). For this purpose, timestamped depth, temperature

and velocity data from the host's tag were extracted and processed using Igor Pro ver. 8.0 (Wavemetrics) and the package of functions Ethographer (Sakamoto et al. 2009).

### 2.3. Mapping remora distribution on sicklefin devil ray bodies

Dorsal and ventral 2-dimensional (2D) representations of sicklefin devil rays (©Marc Dando, with permission) were georeferenced using ArcMap (ESRI 2011). For the base map (i.e. devil ray illustration), the midpoint of the rostral margin was set as the origin of the coordinates (0,0), and DW, DL, cranial width and head length measurements were scaled up according to the relative measurements available (Notarbartolo di Sciarra et al. 1987) based on a DW of 3000 mm. The World Mercator  $x,y$  coordinate system was used as a spatial reference with meter and degree as linear and angular units, respectively.

Using the recorded videos during the surveys (see Section 2.2.1 for more details on the data extraction), we visually identified the position of each remora ( $n = 1121$ , attached or hovering) on the ventral and dorsal sides of the sicklefin devil ray. The positions of the remoras and the suction marks were plotted in the georeferenced models along with an estimated degree of certainty for each observation, from lower to higher, where 1 denotes the head of the remora is not visible, 2 denotes the remora is blurry but the head is visible and 3 denotes a sharp view of the remora. The remoras were semi-quantitatively classified into 2 size categories using their size relative to the host's DL (for dorsal images) or host's rostrum to cloaca length (for ventral images) (Notarbartolo di Sciarra 1987) and considering the remora as small (<10%) or large (>10%) relative to the host size (Wingert et al. 2021).

Georeferenced  $x,y$  coordinates were then obtained for each point using Arc ToolBox (ESRI 2011). Dorsal and ventral representations of the sicklefin devil ray were divided into 5 sectors, from the head to the tail, to describe the distribution and abundance of attached remoras (Fig. 1B).

## 2.4. Computational fluid dynamics (CFD)

### 2.4.1. Geometry and simulation scenario descriptions

Publicly available 3D models of the oceanic manta ray *Mobula birostris* and remora *Echeneis naucrates* from the 3D CAD Browser platform (<https://3dcadbrowser.com/>) were adapted to match the video and pictures of free-swimming sicklefin devil rays and common remoras along with measurements derived from stereophotogrammetry and comments from the authors (B. C. L. Macena and J. M. R. Fontes). Accordingly, the sicklefin

devil ray body was dimensioned (Notarbartolo di Sciarra 1987) to build a 3D model with the following dimensions: DL = 1680 mm and DW = 3000 mm.

For the remora, the SLs of small and large specimens were set to 120 and 480 mm, respectively (Sanches 1991). The average speed reference from a slow gliding to a fast swimming sicklefin devil ray ranged between 0.75 and 4.00  $m s^{-1}$ , respectively (Thorrold et al. 2014, Fontes et al. 2022). The positions of the remora to run the hydrodynamic simulations were chosen post hoc based on the remora's most frequent spatial distribution around their host, either attached or in hovering configurations (present study). The simulation model scenarios were as follows: Scenario 01, small remora attached to the tail; Scenario 02, large remora attached to the anterior dorsal side; Scenario 03, large remora attached to the anterior ventral side; and Scenario 04, large remora hovering under the posterior ventral side (Fig. 1C, Table 1).

### 2.4.2. CFD simulation setup

Numerical simulations were performed using the commercial CFD software ANSYS Fluent (Ansys® Academic Research Mechanical, Release 18.1). The domain for all simulations follows the same shape and boundary conditions (Xu et al. 2021) and was scaled based on the characteristic length of the largest body present in the domain, i.e. the devil ray (Fig. S1 in the Supplement at [www.int-res.com/articles/suppl/m752p117\\_supp.pdf](http://www.int-res.com/articles/suppl/m752p117_supp.pdf)). A steady-state Reynolds-averaged Navier-Stokes model and a  $k-\epsilon$  realizable turbulence model were chosen for this study with scalable wall functions to improve results on low-velocity regions. The model used constant fluid properties corresponding to seawater at 20°C ( $\rho = 1025 \text{ kg m}^{-3}$  and  $\mu = 0.00109 \text{ Pa}$ ). The Reynolds numbers (Xu et al. 2021) calculated for each scenario are presented in Table S1.

A grid independence analysis for free-swimming remoras and sicklefin devil rays was conducted to verify

Table 1. Scenarios used in computational fluid dynamics (CFD) simulation models, describing the model reference, remora size, body region and position simulated. Remora size: relative size to the host's disc length or rostrum to cloaca length, small <10% and large >10%

Model	Size	Mobility	Region	Position
Scenario 01	Small	Attached	Dorsal	Tail
Scenario 02	Large	Attached	Dorsal	Head
Scenario 03	Large	Attached	Ventral	Under mouth
Scenario 04	Large	Hovering	Ventral	Lower pectoral

the accuracy of the numerical simulation (Xu et al. 2021). Minimum variation between the fine mesh and the very fine mesh for both devil rays and remoras was observed (Table S2). Therefore, fine mesh parameters were chosen to reduce computational processing time.

#### 2.4.3. Hitchhiker and host hydrodynamic simulations

The hydrodynamic performance of the gliding motion of the sicklefin devil ray alone and with remoras attached or hovering at different positions around the host (Fig. 1C, Scenarios 01–04) was investigated by extracting velocity contours and vectors in the midsection, static pressure and shear stress contours on the body. We reported absolute pressure and shear stress forces (in Pa) acting on the surface of the model in the direction of the flow, representing pressure and viscous drag, respectively. The total drag force was then calculated by summing both pressure and viscous drag. The negative sign of the drag force equates to a force contrary to the motion of the model species. Vorticity isosurfaces were calculated based on the  $Q$ -criterion for vorticity to have a general idea of the regions of high vorticity.

The relative drag variation on the sicklefin devil ray's surface resulting from the positioning of the remoras in the 4 scenarios (Fig. 1C, Table 1) was calculated as the percentage of drag added by the remora to the free-swimming devil ray body drag for the same water flow velocities. Similarly, the relative drag change on a free-swimming remora resulting from hitchhiking at different locations on the devil ray surface was calculated as the percentage of drag added by being attached to or hovering around their host to the free-swimming remora body drag.

#### 2.5. Data analysis

The kernel density function (Silverman 1986) was used to calculate the probability density distribution of point features (i.e. remoras) in the dorsal and ventral 2D sicklefin devil ray representations using Arc ToolBox (ESRI 2011). Only coordinates with a higher degree of certainty (i.e. 2 and 3) were used. The cell size for the output raster dataset was set to match the georeferenced image of the devil ray, and the search radius (or bandwidth) was set to include all points (remoras) within a 0.1 m neighbourhood. The units were based on the linear unit of the projection of the output spatial reference (i.e. metres). Output values

were converted to the number of remoras per square metre corresponding to the 5, 25, 50, 75 and 95% of the total point features (remoras) probability.

The relative frequency and distribution of remoras and suction marks were determined from the dorsal and ventral sides of sicklefin devil rays swimming close to the surface ( $n = 722$ ) and exported from the attribute table in ArcGIS. To test whether the relative abundance of remoras according to the type of interaction (attached/hovering) or size (small/large) on the ventral and dorsal sides was independent of being on the right or the left side, 2-tailed  $p$ -values for the 2 categorical variables were calculated with Fisher's exact test. We used a chi-square contingency test with multiple categorical variables (5 sectors, Fig. 1B) to test if the abundance of attached/hovering or small/large remoras differed between sectors on the dorsal and ventral sides of the sicklefin devil ray. The statistical analyses were performed using GraphPad Prism ver. 8 (GraphPad Software) and R programming (R Core Team 2022). All measurement metrics are presented as mean  $\pm$  SD and 95% CI.

### 3. RESULTS

#### 3.1. Sicklefin devil ray and remora body measurements

The mean sicklefin devil ray DL with accurate stereophotogrammetry measurements ( $n = 76$ ) was  $1752.1 \pm 131.4$  mm (95% CI: 1722.0–1782.1; range: 1455.3–2124.8) for both genders pooled. The 13 fully measured (DL + DW) sicklefin devil rays allowed the calculation of the first accurate length–width (DL vs. DW) relationship (see Section 2.2.2 for details) for the species, thus resulting in an estimated mean DW of  $2794.4 \pm 178.0$  (95% CI: 2753.7–2835.1; range: 2392.4–3299.4;  $n = 76$ ). The SL for remoras with accurate stereophotogrammetry measurements ( $n = 46$ ) was  $432.9 \pm 108.6$  mm (95% CI: 400.7–465.2; range: 147.5–601.6).

A subset of the stereophotogrammetry database where both the remoras (on the dorsal or ventral side) and the sicklefin devil rays were concurrently measured ( $n = 35$ ) was used to compare the relative body size of both animals. This resulted in a proportion of the symbiont (remora:  $SL_{\text{mean}} = 401.9$  mm;  $SL_{\text{max}} = 601.6$  mm) to the host (devil ray:  $DL_{\text{mean}} = 1752.07$  mm;  $DL_{\text{max}} = 2124.82$  mm) mean and maximum body size relationship (i.e. remora size compared to devil ray size) of 22.9 and 28.3%, respectively. Thus, the relative size of the remoras was predominantly large (>10%) compared to the host's size.

### 3.2. Remora frequency and distribution on sicklefin devil ray

The common remora *Remora remora* was the predominant hitchhiker positively identified in the survey videos (40.6%;  $n = 455$  of 1121), and due to the quality of the images (i.e. focus, light, distance from camera), the remaining remoras were only identified to genus level as *Remora* sp. since both the other Echeneidae genera, *Phtheichthys* and *Echeneis*, can be clearly distinguished from *Remora* by their very slender elongated body (Whitehead 1984). *R. remora* (Fig. S2) was visually identified by colouration (light greyish to dark brown, distinct from *R. albescens*); elongated but robust body (*R. brachyptera* has a slender body); pelvic fins long, pointed and broadly attached to the belly (distinguished from *R. australis* and *R. osteochir* by the head shape and/or suction cup proportion to the head; *R. albescens* pelvic fins are broad, rounded and joined to the belly); and, finally, cephalic disc reaching the posterior end of the pectoral fins, while in the other species, this proportion is different (Collete 2002). In addition, 8 remora specimens were collected from sicklefin devil rays at the same aggregation under a parallel study, and all were identified as *R. remora* (J. M. R. Fontes unpubl. data). Nevertheless, we cannot disregard that remora species other than *R. remora* also attach to the sicklefin devil rays.

The majority of sicklefin devil rays had at least 1 hitchhiking remora (98.8%;  $n = 342$  of 346), and hitchhiker absence was a rare event (1.2%;  $n = 4$  of 346). Considering only devil rays for which at least 75% of its total body surface was visible ( $n = 51$ ), they often carried 2 (50.9%;  $n = 26$ ) or 3 (25.5%;  $n = 13$ ) and sometimes up to 4 ( $n = 2$ ) or 5 ( $n = 1$ ) remoras. Sicklefin devil rays carried an average of  $2.45 \pm 0.90$  (95% CI: 2.20–2.70) hitchhikers, commonly distributed as 1 remora on the dorsal side (mean = 1.47; 95% CI: 1.4–1.53), 2 remoras on the ventral side (mean = 1.65  $\pm$  0.63; 95% CI: 1.58–1.73) and 1 remora on the tail (mean = 1.25  $\pm$  0.48; 95% CI: 1.12–1.38).

Remoras showed no bilateral preference for either the dorsal or ventral sides of the host when comparing attached/hovering on the dorsal side (2-sided Fisher test:  $F = 0.9957$ , 95% CI: 0.4307–2.302,  $p > 0.9999$ ), large/small on the dorsal side ( $F = 1.014$ , 95% CI: 0.4373–2.351,  $p > 0.9999$ ) and attached/hovering on the ventral side ( $F = 0.7747$ , 95% CI: 0.5471–1.095,  $p = 0.1570$ ). In contrast, we found differences in the remora distribution from the head to the tail sectors (chi-square test: attached/hovering on the dorsal side  $\chi^2 = 132.5$ ,  $p < 0.0001$ ; large/small on the dorsal side

$\chi^2 = 458.0$ ,  $p < 0.0001$ ;  $\chi^2 = 322.6$ ,  $p < 0.0001$ ; and attached/hovering on the ventral side and large/small on the ventral side  $\chi^2 = 47.6$ ,  $p < 0.0001$ ).

Based on the qualitative measurements (i.e. body size proportion), of the 1121 remora records, 82.7% were large sized relative to the host ( $n = 927$ ; Fig. 2) and showed a preference for anterior attachment sectors (dorsal and ventral sector 1; 53.5% of the total remora observations,  $n = 600$ ; Figs. 2A, 3B & 4B). When large-sized remoras were hovering ( $n = 206$ ), the majority of those were positioned on the ventral side of sector 3 close to the body core (71.4% of the large hovering remora observations,  $n = 147$ ; Figs. 2B & 4D). Small remoras ( $n = 184$ ) were found attached on the dorsal side of the tail, behind the dorsal fin (56.5% of the small remora observations,  $n = 104$ ; Figs. 2A, 3C & 4C). In addition, we found that the remoras attached to the tail were relatively smaller than the ones on any other sector of the dorsal or ventral sides. However, only 1 individual attached to the tail could be accurately measured with stereophotogrammetry (117.99 mm SL), limiting further analysis of their distributional patterns. When small remoras were hovering ( $n = 43$ ), they were mostly present on the ventral side of sector 3 (62.8% of the small hovering remora observations,  $n = 27$ ; Fig. 4D), similar to hovering large remoras.

Suction marks accounted for 162 records, of which 150 (92.6%) and 12 (7.4%) were on the dorsal and ventral sides, respectively (Fig. 2C). Suction marks on the dorsal side were predominantly located on dorsal sector 4 (53.7%;  $n = 87$ ), even though no attached remoras were observed overlying the suction marks, especially close to the dorsal fin (Figs. 3A & 4A).

### 3.3. Sicklefin devil ray hydrodynamics

Hydrodynamic simulations for velocity contours (Fig. S3), pressure drag, friction drag and vortex iso-surfaces (Fig. 5A,B,C, respectively) were calculated for sicklefin devil rays at  $0.75 \text{ m s}^{-1}$  swimming speed. The stagnation regions of the flow appear at the foremost point at the head, whereas as the flow reaches the highest point in the middle of the dorsal side, it reaches its highest free-stream velocity (Fig. S3).

Regions with the lowest pressure (Fig. 5A) correspond to regions with the highest free-stream velocity (Fig. S3). Wall shear stress is lower on the posterior part of the body and some regions around the head (Fig. 5B), and the higher intensity vortices (purple) on both the ventral and dorsal regions (Fig. 5C) indicate the structure of the flow (Flammang et al. 2020). Vor-

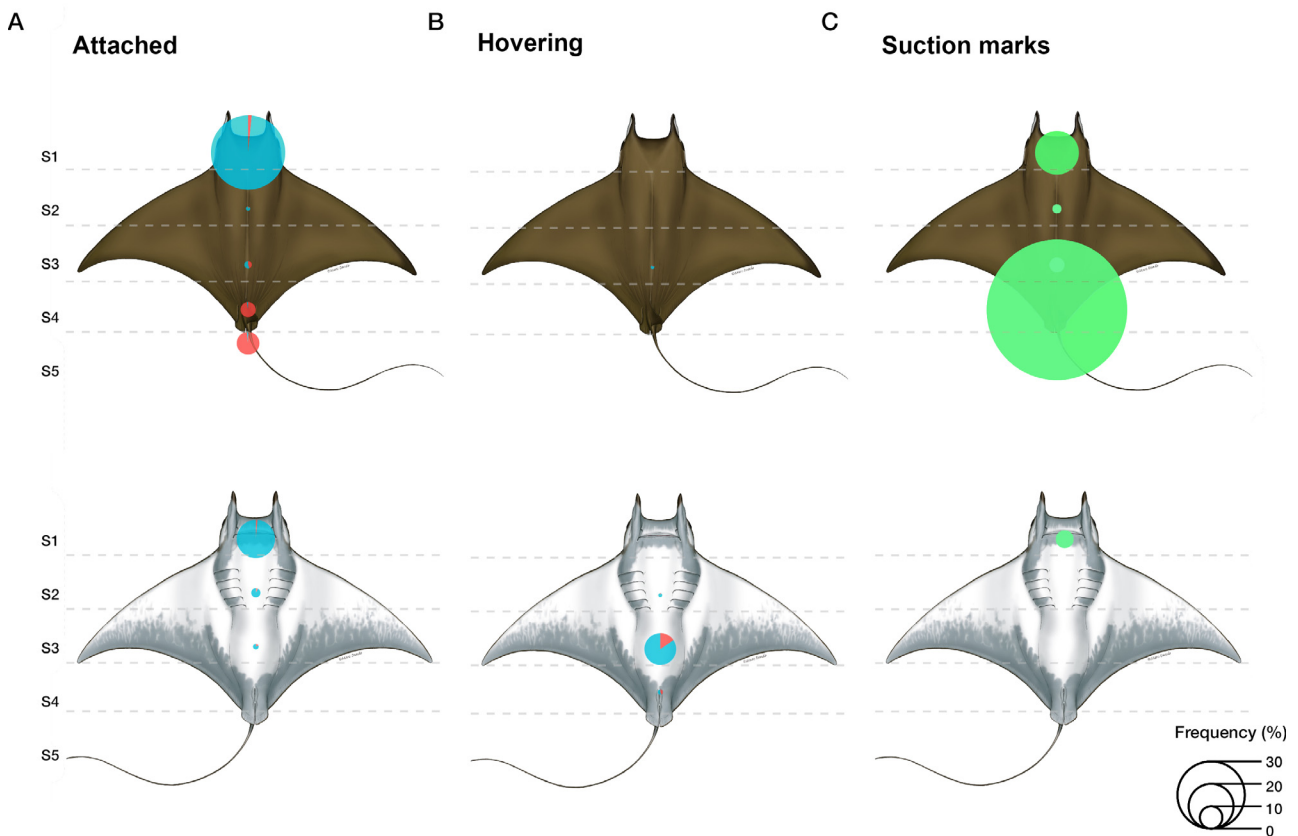


Fig. 2. Relative frequency of (A) attached and (B) hovering remoras pooled by size (blue = large; red = small) and (C) relative frequency of suction marks only (green) for the dorsal (top) and ventral (bottom) sides distributed by sector (S1–S5). Remora size: relative size to the host's disc length or rostrum to cloaca length, small <10% and large >10%. Image ©Marc Dando, with permission

tex core regions map well with the higher shear stress regions and designate the regions where turbulent kinetic energy is higher and present more fluctuations in the average velocity, justifying the low remora frequency in these regions.

#### 3.4. Resistive forces of swimming sicklefin devil rays with remoras

Values of the resistive forces (i.e. static pressure, skin friction and total drag) for sicklefin devil rays and remoras at different positions (i.e. model scenarios, Fig. 1C) on the host are presented in Table 2. The percentage of drag variation (i.e. increase/reduction drag) was calculated for both the host and hitchhiker to assess the variation of drag forces when the remoras are located at different positions on the devil ray's body.

The preferential location for small remoras at the dorsal side of the tail (Scenario 01) showed the highest drag reduction for the remora and the lowest drag

for the devil ray (Table 2). Since the remora is attached in a flow-separated region, the flow velocity magnitude is lower and changes direction (Fig. 6, Scenario 01), thus explaining the decrease of drag for the remora as well as the direction of the force. The most common attachment on both dorsal and ventral sides (Fig. 6, Scenarios 02 and 03, respectively) and hovering (Fig. 6, Scenario 04) positions of the remora showed a drag reduction for the hitchhiker (Table 2). Conversely, the highest added drag experienced by the host (Scenario 02) was estimated to be 4.1% relative to the hitchhiker-free devil ray scenario (Table 2). The presence of the remora in Scenario 02 extends the area of high pressure on the devil ray (Fig. 6, Scenario 02). Therefore, in Scenario 02, the increase in pressure drag explains the higher total drag for both the remora and the devil ray. On the other hand, in Scenario 03, the remora experiences a decrease in pressure drag and consequently in total drag, as this attachment position is more favourable for the remora (Table 2; Fig. 6, Scenario 03). Since the remoras were always observed side by side (i.e. not

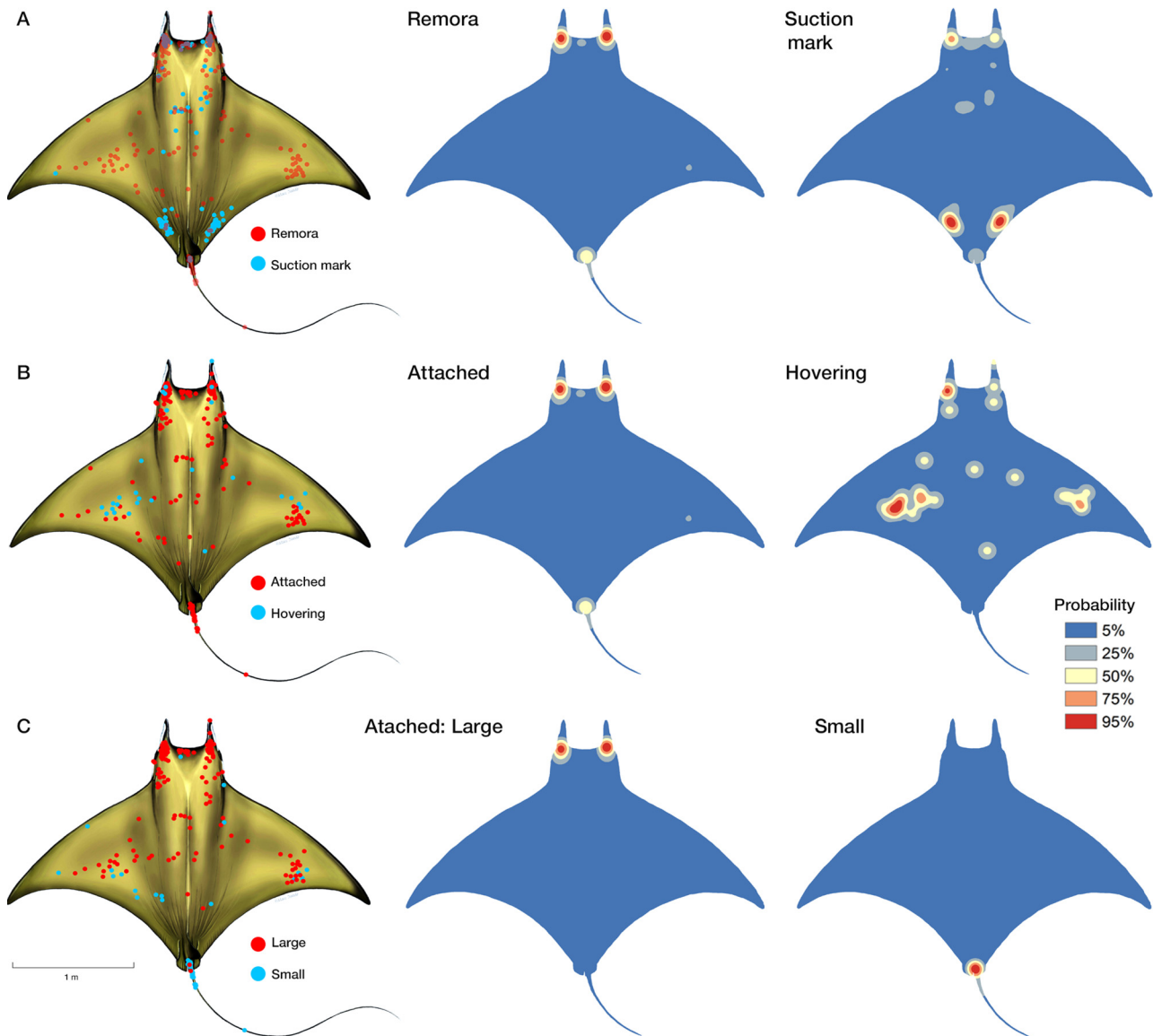


Fig. 3. Distribution of remoras on the dorsal side of sicklefin devil rays (left) and kernel density map (mid and right) for (A) remoras and suction marks, (B) remoras attached and hovering and (C) pooled large and small remoras for both attached and hovering. Remora size: relative size to the host's disc length or rostrum to cloaca length, small <10% and large >10%. Probability (kernel density map) is represented in 5 relative categories corresponding to the 5, 25, 50, 75 and 95% of remoras per square metre (coloured from blue to red/top to bottom, respectively). A total of 416 dorsal images of sicklefin devil ray were processed, and only observations with a degree of certainty  $\geq 2$  were considered

anteroposteriorly aligned in the dorsal or ventral region) on the host, the net drag from additional hitchhikers was considered to have linear increase; thus, each large remora attached to a sicklefin devil ray's dorsal side sums ca. 4.1% of drag (e.g. 2 remoras would have a net drag of ca. 8.2%).

Additionally, we looked at the animal-borne tagged sicklefin devil rays which performed deep dives (>400 m;  $n = 6$ ), to confirm the presence of remoras associated with these deep-diving hosts ( $n = 5$ ) either by

observing the remora at depth ( $n = 4$ ) or by observing the remora before and after the dive in the same position ( $n = 1$ ). Remoras were observed attached to the host during the fastest descent ( $\sim 5 \text{ m s}^{-1}$ ) in 1 of the deep dives (Fig. 7). Therefore, we quantified the impact of an increase in free-stream velocity to  $4.0 \text{ m s}^{-1}$  on the total drag for the remora and the devil ray in Scenario 02, which had the highest drag penalty for both. The drag variation for the remora and the sicklefin devil ray when attached to the host in this position

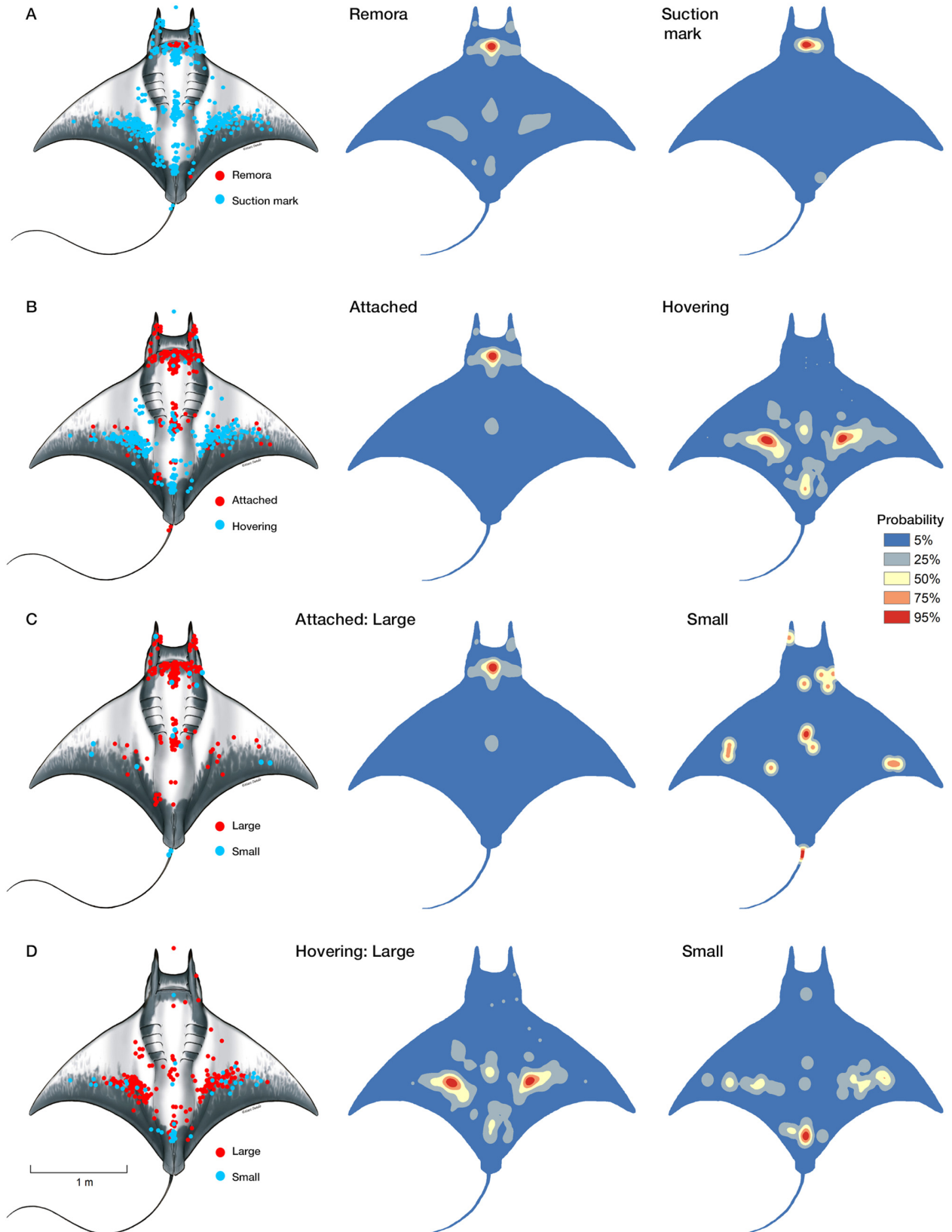


Fig. 4. Distribution of remoras on the ventral side of sicklefin devil rays (left) and kernel density map (mid and right) for (A) remoras and suction marks, (B) attached and hovering remoras, (C) attached large and small remoras and (D) hovering large and small remoras. Remora size: relative size to the host's disc length or rostrum to cloaca length, small <10% and large >10%. Probability (kernel density map) is represented in 5 relative categories corresponding to the 5, 25, 50, 75 and 95% of remoras per square metre (coloured from blue to red/top to bottom, respectively). A total of 307 ventral images of sicklefin devil rays were used, and only observations with a degree of certainty  $\geq 2$  were considered

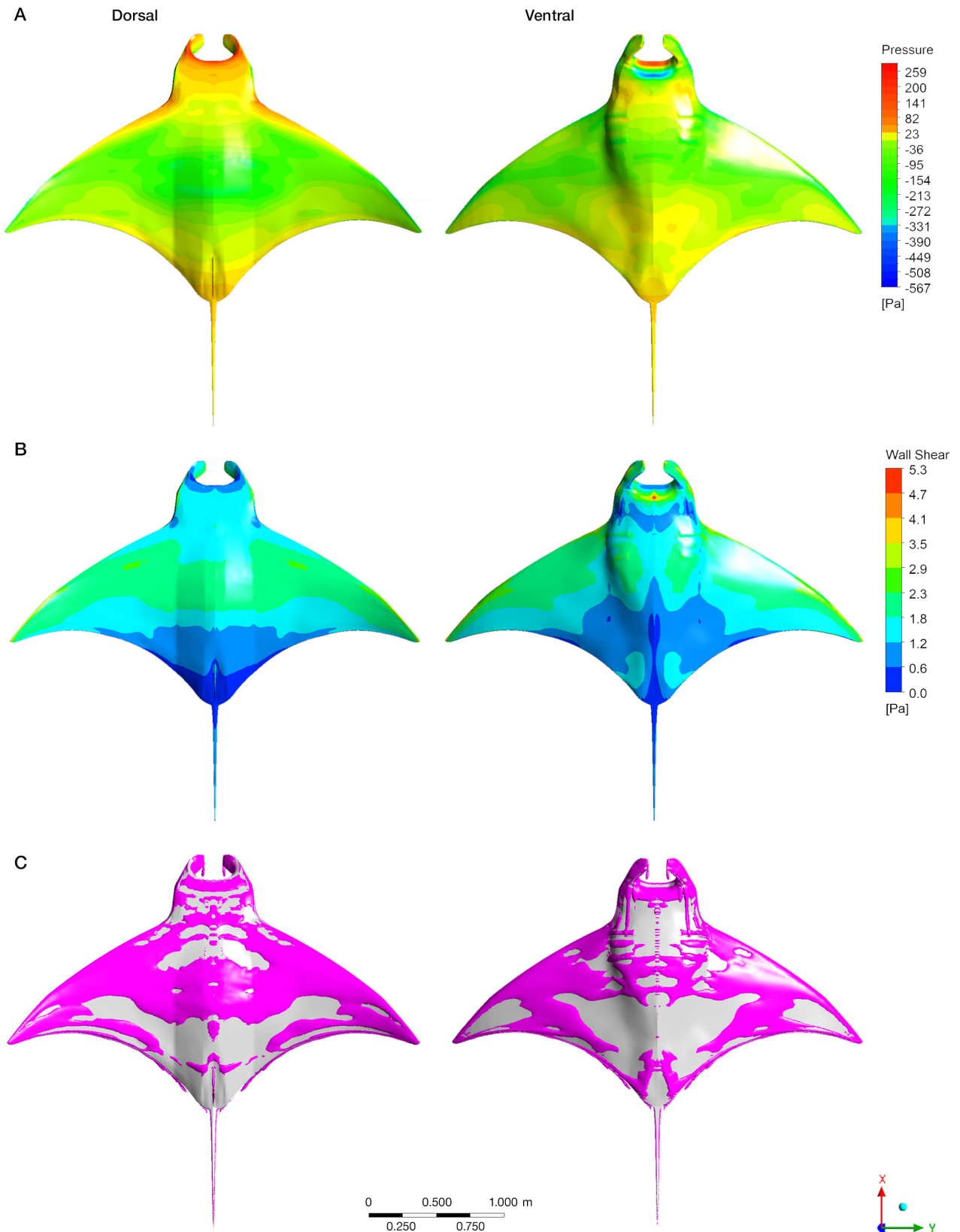


Fig. 5. Hydrodynamic profile of sicklefin devil rays free swimming at low speed. (A) Pressure contours displayed on the surface of the model and coloured by absolute pressure. (B) Friction drag on the dorsal and ventral sides displayed as wall shear stress and coloured by pressure. (C) Vortex isosurfaces on the dorsal and ventral surface, displayed as vorticity field; higher intensity vortices (purple) indicate the structure of the flow

Table 2. Drag for sicklefin devil rays alone and with remoras attached and hovering at different body locations and velocities. Pressure, skin friction and total drag for the remoras and devil rays in the combined devil ray and remora scenarios (in N) and the associated increase or decrease (%) in devil ray plus remora total drag. See Table 1 for scenario details. Velocity (Vel.) is expressed in  $\text{m s}^{-1}$ . Remora size: relative size to the host's disc length or rostrum to cloaca length, small (S) <10% and large (L) >10%

Model	Vel.	Devil ray			Remora				Devil ray + remora		
		Pressure drag	Skin friction drag	Total drag	Size	Pressure drag	Skin friction drag	Total drag	Total drag	Devil ray drag increase	Remora drag decrease
Remora	0.75				S	-0.018	-0.013	-0.031			
Remora					L	-0.237	-0.196	-0.433			
Devil ray		-6.009	-7.685	-13.694							
Scenario 01		-6.002	-7.676		S	0.004	-0.001	0.003	-13.675	0.000	109.680
Scenario 02		-6.200	-7.636		L	-0.292	-0.127	-0.419	-14.255	4.090	3.230
Scenario 03		-6.360	-7.641		L	0.136	-0.159	-0.023	-14.024	2.400	94.750
Scenario 04		-6.015	-7.861		L	-0.172	-0.170	-0.342	-14.038	2.500	21.050
Remora	4.00				L			-10.500			
Devil ray				-305.490							
Scenario 02				-310.281	L			-10.294	-310.281	4.940	1.960

slightly increased with the intensification in swimming speed (from  $-3.23$  to  $-1.96$  and from  $4.10$  to  $4.94\%$ , respectively), despite the absolute increase in drag for both when swimming speed increased (Table 2).

#### 4. DISCUSSION

The understanding of remora–host ecology is limited by difficulties in obtaining systematic observations of their interactions in the open ocean. As a result, only a few studies describing this association exist to date, and they are typically derived from opportunistically collected data (Silva & Sazima 2003, Brunnschweiler & Sazima 2008, Brunnschweiler et al. 2020) or are only about the remora's physics/mechanics of the suction cup/attachment mechanism (Beckert et al. 2015, Flammang & Kenaley 2017). Thus, seasonal yet predictable oceanic aggregations of hosts, such as the one of the sicklefin devil rays studied here, offer a unique opportunity to investigate this largely understudied topic. This is the first study that investigated the remora distribution and population structure, the host's hydrodynamic costs and the implications of the endangered sicklefin devil ray and remora ecological interaction.

##### 4.1. Distribution, hydrodynamics and costs for the hitchhikers

Remoras were extremely common hitchhikers on the sicklefin devil rays, with about 1% of the devil rays not having at least 1 associated remora. In addition,

we observed that remoras select specific attachment and hovering positions relative to the host's body, and this preference changes ontogenetically. The ubiquity and geographical specificity of this interaction thus strongly suggest that it is ecologically relevant for both species (Mougi 2016), regardless of the ecological nature of their symbiosis (i.e. mutualistic, commensalistic or parasitic) (Mathis & Bronstein 2020).

Remoras were typically found attached or hovering at specific host sectors, which generally correspond to regions of reduced overall drag (Flammang et al. 2020). The significance of this strategy may be 2-fold, as the cost of transport for the hitchhiker is reduced or transferred to the host, while the added load on the host is kept lower than if remoras were randomly distributed or if they prefer regions with high drag on the surface of the host. A similar distribution pattern was also observed on a larger host such as baleen whales (Flammang et al. 2020).

In streamlined host bodies (i.e. reduced form drag) such as devil rays, almost the entire fluid resistance is caused by frictional drag (Munson et al. 2006). In agreement, regions with higher frequencies of attached large remoras overlapped with the sections where predicted shear stress is reduced (i.e. lower frictional drag) independently of the boundary layer thickness. Nonetheless, the relatively small thickness of the boundary layer on the posterior sectors of the ray can cover 24% of a large remora's diameter (Beckert et al. 2016), which may contribute to reducing drag for remoras and minimising the cost of transport for hosts as well. In the anterior part of the dorsal side, this reduction is lower because pressure has a higher impact on the drag; however, since the remora's

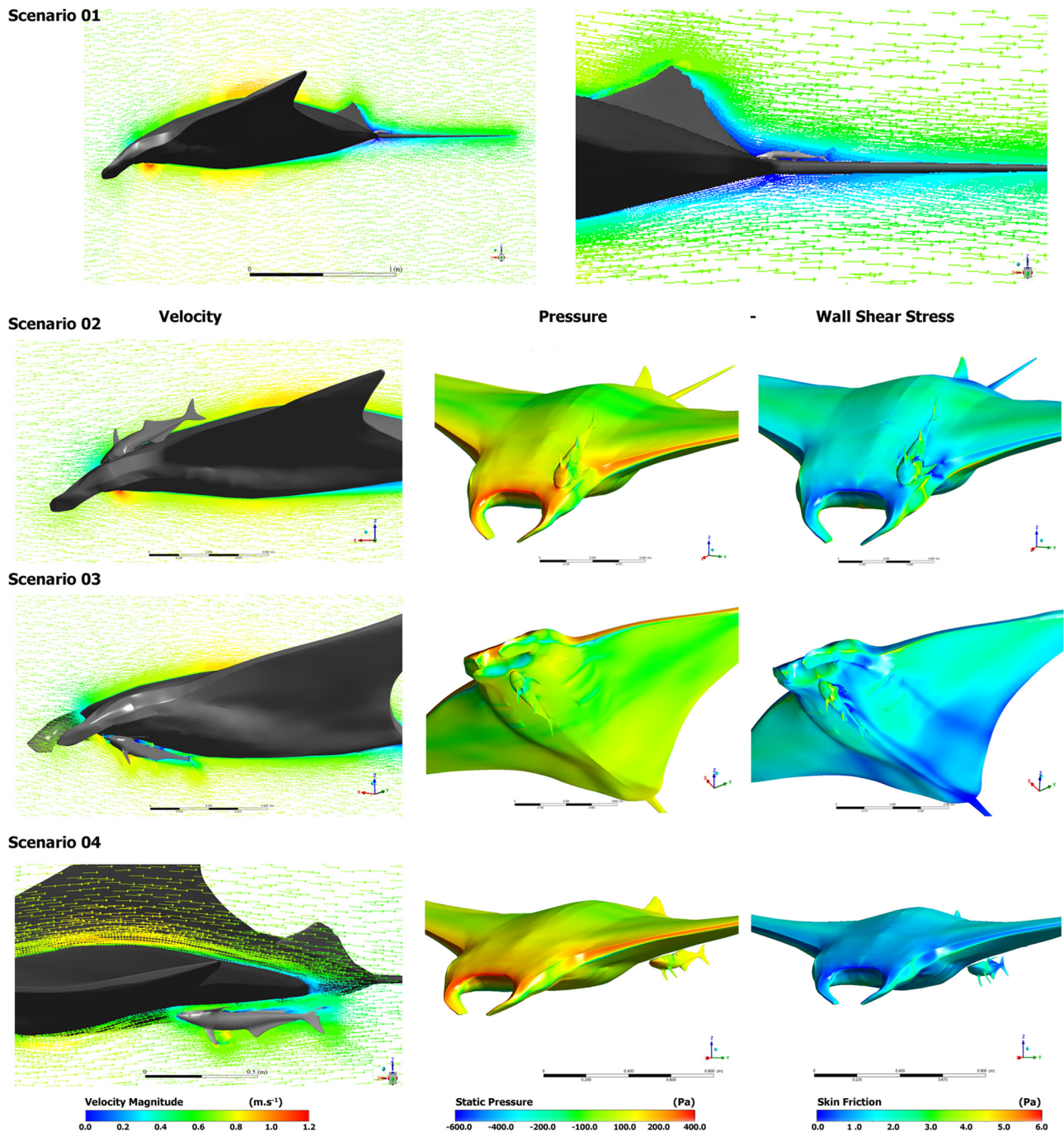


Fig. 6. Fluid drag experienced by the host and hitchhiker in some of the most common attachment positions at low speed. Velocity vectors profile (left panel), pressure (mid panel) and wall shear stress (right panel) drag contours on the dorsal and ventral sides displayed on the surface of the model and coloured by velocity magnitude (in  $\text{m s}^{-1}$ ), absolute static pressure (in Pa) and skin friction (in Pa) for each scenario (rows). For Scenario 01, only the velocity vector is shown. The boundary layer thickness is 6 mm

adhesion is enhanced by friction through the spinules on the dorsal pad lamella (Beckert et al. 2016), attaching to regions with lower shear stress may reduce the tensions in the remora itself and thus be more favourable than lower pressure regions.

Small remoras showed a distinct distribution compared to large remoras, predominantly attaching to the tail behind the dorsal fin. In this case, the 6 mm thick boundary layer observed in that region of the sicklefin devil ray and the wake created by the dorsal

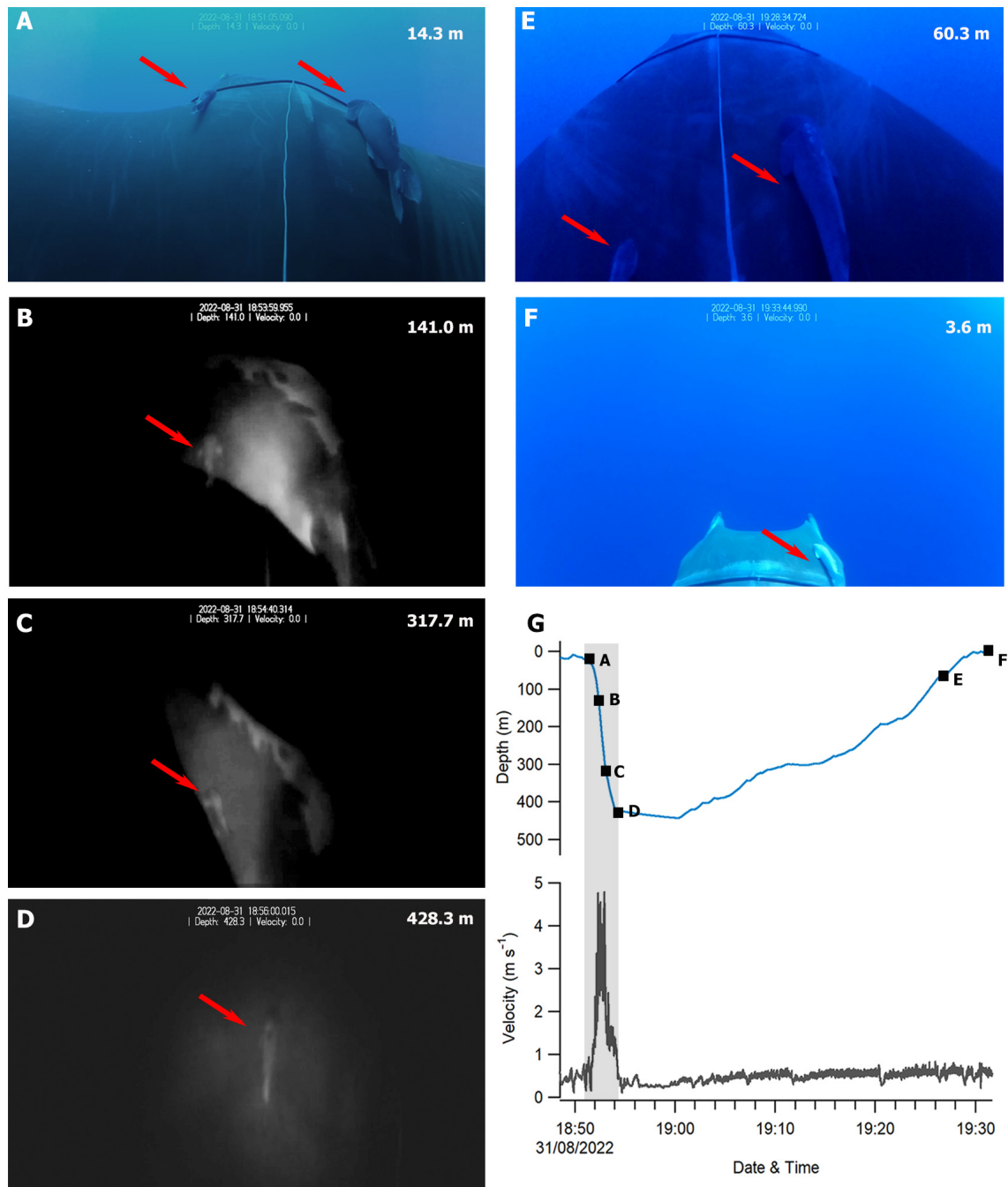


Fig. 7. Association of remoras to their host. (A–F) Remoras recorded during the deep power dive on the dorsal side, during the descending fast acceleration ( $\sim 5 \text{ m s}^{-1}$ ) on the ventral side and at 428 m depth on the dorsal side then back to the surface. Images refer to the video frames recorded by the i-Pilot tag (Fontes et al. 2022). Red arrows indicate the remoras attached on the host before and after the dive. (G) Depth and velocity profiles of a 45 min deep dive ( $>400 \text{ m}$ ). The shaded area indicates the power dive (from 14 to 428 m depth)

fin (Flammang et al. 2020) is enough to shelter the small remora from free-stream conditions but not for larger remoras. Our CFD simulations confirm that small remoras attached to the tail may be experiencing drag forces close to zero. This may also indicate a

consequence of competition for space, since larger remoras should dominate and occupy the best remaining spots (i.e. with less drag) on the devil ray's body (Figs. 3 & 4) but cannot attach to the tail due to their size. Alternatively, the smaller remoras could

also use other restricted spaces such as inside the cloaca and gill slits as a shelter from predation either by larger remoras or by other fishes.

In contrast, hovering remoras were observed in low-turbulence regions with little or no vortex formation above (less frequent) or under (more frequent) the host (Fig. 4D), as the steadier flow should help maintain the remora positioning (Fig. 6, Scenario 04). Although hovering remoras may benefit from drag reduction, hovering should still be energetically more expensive compared to attachment mode, and it is unclear why hovering is sometimes preferred and what specific function it serves. One hypothesis is that hovering could promote easier (faster) access to prey. This seems to be supported by previous observations that large associated remoras feeding on small pelagic fishes (Stewart et al. 2018, Solleliet-Ferreira et al. 2020) preferred the ventral hovering position relative to the dorsal head attachment mode when their devil ray hosts charged at prey (Fig. S4). Even though our results suggest that remora attachment location preferences may be mostly driven by an energy-saving strategy, they may also favour other vital functions with some implications to the remora energy budget, such as passive gill respiration. Remora passive respiration is thought to be more efficient when water flows into their mouth at slow speeds of  $0.60 \text{ m s}^{-1}$  (Muir & Buckley 1967). With sicklefin devil rays typically swimming at lower speeds on the Azorean shallow aggregations (Fontes et al. 2014, Sobral & Afonso 2014), passive respiration and reduction of the respiration energy cost of the remora may thus be enhanced by attaching to host sections with higher free-stream velocities, such as over the head.

The attachment preferences may also serve to minimize the probability of dislodgement by minimising the added cost of transport, staying away from sensitive areas and not interfering with the host's behaviour (Silva & Sazima 2008, Beckert et al. 2015, Brunnenschweiler et al. 2020, Wingert et al. 2021). In addition, remoras were frequently observed in attachment locations where the underlying muscles have lower deformation capacity to prevent dislodgement by muscle contraction underneath the attachment that may disrupt the suction seal (Fulcher & Motta 2006, Flammang & Kenaley 2017). Nevertheless, the attachment site preference of the remoras also adds the cost of an injury (i.e. physical abrasion from the suction) to the hosts (Brunnenschweiler et al. 2020). When remoras attach themselves to the posterior sectors of a devil ray, they normally cause a repeated undulating shivering-like response from their host; such annoyance response behaviour is also observed in

other species (Silva & Sazima 2008, Weihs et al. 2007). Large remoras favour anterior attachment sectors away from the eyes, where either they do not trigger a host response or the host has lower contraction capability. Nonetheless, the consistent presence of suction marks close to the dorsal fin, where attached remoras have been rarely observed, remains to be explained.

#### 4.2. Ecological significance of remora–devil ray association

Apart from previous evidence for the improved feeding hypothesis for hovering remoras, hitchhiking may play an important role in remora reproduction (Battaglia et al. 2016) and provide a mobile nursery ground for remora offspring (Sheaves et al. 2024). Our data show that most of the remoras were large and had potentially reached maturity (Bachman et al. 2018) and that 2 or more remoras are typically associated with 1 aggregating devil ray (i.e. mating pairs). When sicklefin devil rays aggregate, remoras have the opportunity to interact and potentially join other mature conspecifics in a different host. In fact, we observed that they sometimes switch hosts, possibly to one with a potential mate, similar to what has been described as mating for the sharksucker (Nakajima et al. 1987).

As streamlined-body fishes, remoras are expected to produce a low hydrodynamic parasitic drag on their host (Beckert et al. 2016), which is in accordance with our CFD simulation results. In the most frequent attachment location, the maximum added drag by a large remora ( $>480 \text{ mm SL}$ ) is  $<5\%$ , at the highest speed tested. Remarkably, smaller remoras do not add drag to their host when located on the tail, for example. When sicklefin devil rays carry more than a single remora, which was typically the case in our study, the flow field impacting one remora can be disrupted by the presence of another remora upstream (i.e. cranial–caudal plane), meaning that the remora-induced drag and the cost of transport for their host will not necessarily increase linearly (Beckert et al. 2016). This was not the case in the most common positions observed in our study, where the added drag increase should be roughly proportionally additive to the total number of remoras. For example, when 3 large remoras are attached simultaneously in the most frequent locations (2 on the anterior dorsal side and 1 on the anterior ventral side), the sicklefin devil ray may experience an approximate drag increase of up to  $12.3\%$  ( $\sim 4.1\%$  of drag from each remora). Simulation studies have shown that the extra effort required by a

large host (e.g. blue whale *Balaenoptera musculus*) to overcome the parasitic drag force of an attached remora is relatively small or even negligible (Flammang et al. 2020). However, this may not be the case for smaller fast-swimming hosts, such as the sicklefin devil ray or other elasmobranchs with smaller body biomass. The total drag increase of a single remora in an oceanic whitetip shark *Carcharhinus longimanus*, at speeds of  $4 \text{ m s}^{-1}$ , can reach 18 to 23%, depending on their position (Xu et al. 2021), which is higher than what we observe for the sicklefin devil ray.

During aggregation at the Azorean seamounts, sicklefin devil rays generally swim at low speeds, and remoras are not always attached to their host. At higher speeds, marine megafauna (including mobulids) manage their energy cost of movement by minimizing the cost of transport (hydrodynamic performance: glide vs. swim) (Weihs & Webb 1983, Fish 1994, Gleiss et al. 2011). The wing stroke swimming motion of mobulids is efficient (89% propulsive efficiency) (Fish et al. 2016), and the large horizontal body surface provides great lift, ideal for gliding even at low speeds. However, the hydrodynamic parasitic drag calculations are likely underestimated on the body of the host because we only simulated the simple case where the host is gliding, i.e. rigid model with no undulating pectoral fin movement. The undulating body motion generates increased shear forces and body drag up to 3-fold (Fish et al. 2016), while the remora drag should remain relatively stable for the same water flow velocity. Devil ray wing stroke movements are frequent and necessary to power any ascent, and sometimes powered descents (i.e. power dives) are also common (Fontes et al. 2022). Nevertheless, swimming efficiency allows a relatively low cost of transport that could minimize the extra drag caused by the transport of remoras on total energy requirements. Therefore, hydrodynamic parasitic drag is likely to have a low impact on the sicklefin devil ray cost of transport and energy budget, especially when swimming at low speeds.

Deep diving or speed bursts have been suggested as a parasite offload strategy by the host (Braun et al. 2022). Still, remoras can accompany their hosts to bathypelagic depths (Fontes et al. 2023), suggesting some degree of host fidelity even after exposure to extreme conditions. Indeed, 1 remora species, the whalesucker *Remora australis*, is known to bond with the spinner dolphin *Stenella longirostris* for almost 3 mo (Silva & Sazima 2003). We have shown that remoras remain attached to sicklefin devil rays during their high-speed descents to a deep dive and that the parasitic drag remains low even at higher swimming

speeds. Noticeably, remoras may prefer favourable positions on the host under these extreme conditions other than those observed at the shallow aggregations, which could explain the suction marks on the posterior dorsal side, where surface pressure and friction drag are low and vortexes are absent. Despite some species displaying specific behaviours as a response to the disturbance from the attachment (Brunnschweiler 2006; present study), such as breaching, to remove the remoras (Ritter 2002, Ritter & Brunnschweiler 2003, Weihs et al. 2007, Klimley et al. 2024), our findings do not support the parasite offload hypothesis through deep diving by the sicklefin devil ray. However, the complexities of these dynamics warrant further investigation.

Additional disadvantages of hydrodynamic drag, including abrasion on the host's skin (Brunnschweiler et al. 2020) and interference with the host's activities (Silva & Sazima 2008), should also be considered. Here, we can only discuss the short-term effects of hitchhikers since, although likely, we cannot confirm if this association persists over the long term. The relatively low parasitic drag and some potential skin abrasions may be an acceptable tradeoff for sicklefin devil rays if remoras provide them with beneficial ectoparasite cleaning services (O'Toole 2002). In fact, the diet of young *R. remora* is highly dependent on the host's ectoparasite copepods and faeces (Cressey & Lachner 1970, Williams et al. 2003). Even though large remoras prey on small pelagic bait fishes (Stewart et al. 2018, Solleliet-Ferreira et al. 2020), both large and small remoras accompany sicklefin devil rays, who should thus benefit to some extent from the cleaning services provided by their younger hitchhikers, especially considering that they undergo extensive migrations (Thorrold et al. 2014). Nevertheless, remoras clearly benefit from this interaction.

In light of the available information and our observations, the costs and benefits of the association for sicklefin devil rays could well be balanced (i.e. no effect), and this association could thus be considered some form of commensalism, i.e. a relationship in which one species (remora) benefits and the other (i.e. devil ray) experiences no net effect. However, if all the remoras associated with sicklefin devil rays were small, the association would shift to be mutualistic (i.e. both species benefit, considering the parasite removal by the remoras), but if the total number of remoras increases or if we consider the long-term increase in the cost of transport of large remoras to be detrimental to sicklefin devil rays, the association could easily become antagonistic (Cushman & Beaty 1991, Leung 2014, Mathis & Bronstein 2020). On

the other hand, if the cost of carrying large remoras, the predominant size observed in the present study, is not detrimental, then the relationship would be parasitic due to the hydrodynamic burden affecting swimming performance. These dynamics are complex and context dependent (Gayford 2024) and need further *in situ* studies to clarify their true ecological nature.

## 5. CONCLUSIONS

Our study provides new insights into the flow fields around sicklefin devil rays and potential links with remora distribution on the host's body. Shear stresses and vortex fields seem to explain well the remora sector attachment and hovering preferences, respectively. Even though the boundary layer is too small to entirely cover a large remora, it is critical to eliminating the drag forces on the smallest individuals. Location selection of remoras on the sicklefin devil ray may be explained by a tradeoff between reduced drag for the remora and other potential biological and ecological benefits (i.e. better access to prey, passive gill respiration or lower dislodgement probability) that could outweigh the cost of transport reduction in specific situations. Information about the relative size of hitchhikers and hosts and the load and distribution of remoras on their host can be used to better assess the energetic cost associated with the transport of remoras and the drag threshold when remoras effectively become hydrodynamic parasites.

**Acknowledgements.** This work received national funds through the Foundation for Science and Technology under projects FCT20006 UIDB/05634/2020 and FCT20007 UIDP/05634/2020 and through the Regional Government of the Azores through the initiative to support the Research Centres of the University of the Azores and through project M1.1.A/REEQ.CIENTÍFICO UI&D/2021/010 and research projects EcoDiveAz (ACORES 01-0145-FEDER-000059), Islandshark (PTDC/BIA-BMA/32204/2017), EcodivePWN (proWIN proNature Foundation), AEROS-Az (ACORES-01-0145-FEDER-000131) and NAUTILOS (101000825 H2020-BG-2018-2020 / H2020-BG-2020-1). J.M.R.F. was co-financed by the operational program AZORES 2020, through the fund 01-0145-FEDER-000140 'MarAZ Researchers: Consolidate a body of researchers in Marine Sciences in the Azores' of the European Union and research grant M3.1.a/F/062/2016 funded by Fundo Regional de Ciência e Tecnologia from Governo dos Açores. G.C.G. was a student in the Marine Environment Erasmus Mundus joint master's degree programme. B.C.L.M. was co-financed by the projects IslandShark, AEROS-Az, MEESO (EU H2020-LC-BG-03-2018) and Mission Atlantic (EU H2020-LC-BG-08-2018-862428). The authors thank Prof. Vincent Hanquiez for his valuable assistance in using ArcGIS and Ricardo Medeiros and Luis Rodrigues for their technical GIS

advice. Special thanks to Betty Laglbauer, Sophie Prendergast, Robert Priester, Bruno Saraiva, Jorge Manuel Moreno Mendoza, Diya Das and Faial, Pico and Santa Maria islands dive operators for providing additional footage. The authors also thank the reviewers for their valuable comments, which improved the quality and comprehension of the manuscript. Research activities were carried out in accordance with the ethics committee protocol of the University of the Azores (UAC/2022/12759) and Azores government permits AMP/2017/013, AMP/2018/015, ELMAS-DRA/2019/05 204 and ELMAS-DRAM/2021/06.

## LITERATURE CITED

- Amin R, Ritter E, Kulldorff M, Barbas A, Schwarzmeier M (2016) Sharksuckers, *Echeneis naucrates*, are non-randomly attached to the bodies of lemon sharks, *Negaprion brevirostris*: a spatial study. *Environ Sci* 4:79–93
- ✦ Bachman BA, Kraus R, Peterson CT, Grubbs RD, Peters EC (2018) Growth and reproduction of *Echeneis naucrates* from the eastern Gulf of Mexico. *J Fish Biol* 93:755–758
- ✦ Battaglia P, Potoschi A, Valastro M, Andaloro F, Romeo T (2016) Age, growth, biological and ecological aspects of *Remora osteochir* (Echeneidae) in the Mediterranean Sea. *J Mar Biol Assoc UK* 6:639–645
- ✦ Becerril-García EE, Gutiérrez-Ortiz MA, Preciado-González PA, Ayala-Bocos A (2020) Presence of *Remora remora* on *Mobula birostris* in Revillagigedo National Park, Mexico. *Mar Freshw Res* 71:414–417
- ✦ Beckert M, Flammang BE, Nadler JH (2015) Remora fish suction pad attachment is enhanced by spinule friction. *J Exp Biol* 218:3551–3558
- ✦ Beckert M, Flammang BE, Anderson EJ, Nadler JH (2016) Theoretical and computational fluid dynamics of an attached remora (*Echeneis naucrates*). *Zoology* 119: 430–438
- ✦ Boutros N, Shortis MR, Harvey ES (2015) A comparison of calibration methods and system configurations of underwater stereo-video systems for applications in marine ecology. *Limnol Oceanogr Methods* 13:224–236
- ✦ Braun CD, Arostegui MC, Thorrold SR, Papastamatiou YP, Gaube P, Fontes J, Afonso P (2022) The functional and ecological significance of deep diving by large marine predators. *Annu Rev Mar Sci* 14:129–159
- ✦ Bray DJ (2019) *Remora albescens*. In: Bray DJ, Gomon MF (eds) *Fishes of Australia*. Museums Victoria and OzFishNet. <https://fishesofaustralia.net.au/home/species/4252/> (accessed 1 Jul 2022)
- ✦ Brunnschweiler JM (2006) Sharksucker—shark interaction in two carcharhinid species. *Mar Ecol* 27:89–94
- ✦ Brunnschweiler JM, Sazima I (2008) A new and unexpected host for the sharksucker (*Echeneis naucrates*) with a brief review of the echeneid—host interactions. *Mar Biodivers Rec* 1:e41
- ✦ Brunnschweiler JM, Vignaud TM, Côté IM, Maljković A (2020) The costs of cohabiting: the case of sharksuckers (*Echeneis naucrates*) and their hosts at shark provisioning sites. *Ecology* 101:e03160
- Collette BB (2002) Echeneidae. In: Carpenter KE (ed) (2002) *The living marine resources of the western central Atlantic, Vol 3: bony fishes part 2 (Opistognathidae to Molidae), sea turtles and marine mammals*. FAO species identification guide for fishery purposes and Am Soc Ichthyologists Herpetologists Spec Publ No. 5. FAO, Rome, p 1414–1419

- ✦ Couturier LIE, Marshall AD, Jaine FRA, Kashiwagi T and others (2012) Biology, ecology and conservation of the Mobulidae. *J Fish Biol* 80:1075–1119
- ✦ Cressey RF, Lachner EA (1970) The parasitic copepod diet and life history of diskfishes (Echeneidae). *Copeia* 1970: 310
- ✦ Cushman JH, Beattie AJ (1991) Mutualisms: assessing the benefits to hosts and visitors. *Trends Ecol Evol* 6:193–195
- ✦ Edwards AJ (1990) Fish and fisheries of Saint Helena Island. Centre for Tropical Coastal Management Studies, University of Newcastle upon Tyne
- ✦ ESRI (Environmental Systems Research Institute) (2011) ArcGIS Desktop: release 10. ESRI, Redlands, CA
- ✦ Fish FE (1994) Influence of hydrodynamic-design and propulsive mode on mammalian swimming energetics. *Aust J Zool* 42:79–101
- ✦ Fish FE, Nicastro AJ, Weihs D (2006) Dynamics of the aerial maneuvers of spinner dolphins. *J Exp Biol* 209:590–598
- ✦ Fish FE, Schreiber CM, Moored KW, Liu G, Dong H, Bart-Smith H (2016) Hydrodynamic performance of aquatic flapping: efficiency of underwater flight in the manta. *Aerospace* 3:20
- ✦ Flammang BE, Kenaley CP (2017) Remora cranial vein morphology and its functional implications for attachment. *Sci Rep* 7:5914
- ✦ Flammang BE, Marras S, Anderson EJ, Lehmkuhl O and others (2020) Remoras pick where they stick on blue whales. *J Exp Biol* 223:jeb226654
- ✦ Fontes J, Schmiing M, Afonso P (2014) Permanent aggregations of a pelagic predator at seamounts. *Mar Biol* 161: 1349–1360
- ✦ Fontes J, Macena B, Solleliet-Ferreira S, Buyle F and others (2022) The advantages and challenges of non-invasive towed PILOT tags for free-ranging deep-diving megafauna. *Anim Biotelem* 10:39
- ✦ Fontes J, Castellano-González G, Macena BCL, Afonso P (2023) Hitchhiking to the abyss. *Ecol Evol* 13:e10126
- ✦ Froese R, Pauly D (eds) (2019) FishBase. [www.fishbase.org](http://www.fishbase.org) (accessed 28 Mar 2022)
- ✦ Fulcher BA, Motta PJ (2006) Suction disk performance of echeneid fishes. *Can J Zool* 84:42–50
- ✦ Gamel KM, Garner AM, Flammang BE (2019) Bioinspired remora adhesive disc offers insight into evolution. *Bioinspir Biomim* 14:056014
- ✦ Gayford JH (2024) The multidimensional spectrum of evolutionary relationships between sharks and remoras. *J Fish Biol* 105:4–9
- ✦ Gleiss AC, Norman B, Wilson RP (2011) Moved by that sinking feeling: variable diving geometry underlies movement strategies in whale sharks. *Funct Ecol* 25:595–607
- ✦ Günther A (1860) XLII. — On the history of *Echeneis*. *Ann Mag Nat Hist* 5:386–402
- ✦ Heemstra PC (1986) Echeneidae. In: Smith MM, Heemstra PC (eds) *Smiths' sea fishes*. Springer-Verlag, Berlin, p 662–664
- ✦ Kenaley CP, Stote A, Ludt WB, Chakrabarty P (2019) Comparative functional and phylogenomic analyses of host association in the remoras (Echeneidae), a family of hitchhiking fishes. *Integr Org Biol* 1:obz007
- ✦ Klimley AP, Curtis TH, Johnston EM, Kock A, Stevens GMW (2024) A review of elasmobranch breaching behavior: Why do sharks and rays propel themselves out of the water into the air? *Environ Biol Fish (Spec Issue Front Elasmobranch Biol)*, doi:10.1007/s10641-024-01584-5
- ✦ Letessier TB, Meeuwig JJ, Gollock M, Groves L and others (2013) Assessing pelagic fish populations: the application of demersal video techniques to the mid-water environment. *Methods Oceanogr* 8:41–55
- ✦ Leung TLF (2014) Fish as parasites: an insight into evolutionary convergence in adaptations for parasitism. *J Zool* 294: 1–12
- ✦ Mathis KA, Bronstein JL (2020) Our current understanding of commensalism. *Annu Rev Ecol Evol Syst* 51:167–189
- ✦ Millar RB, Anderson MJ (2004) Remedies for pseudoreplication. *Fish Res* 70:397–407
- ✦ Morato T, Varkey DA, Damaso C, Machete M and others (2008) Evidence of a seamount effect on aggregating visitors. *Mar Ecol Prog Ser* 357:23–32
- ✦ Mougi A (2016) The roles of amensalistic and commensalistic interactions in large ecological network stability. *Sci Rep* 6:29929
- ✦ Muir BS, Buckley RM (1967) Gill ventilation in *Remora remora*. *Copeia* 1967:581–586
- ✦ Munson BR, Young DF, Okiishi TH (2006) *Fundamentals of fluid mechanics*. J. Wiley & Sons, Hoboken, NJ
- ✦ Nakajima H, Kawahara H, Takamatsu S (1987) The breeding behavior and the behavior of larvae and juveniles of the sharksucker, *Echeneis naucrates*. *Jpn J Ichthyol* 34:66–70
- ✦ Nicholson-Jack AE, Harris JL, Ballard K, Turner KME, Stevens GMW (2021) A hitchhiker guide to manta rays: patterns of association between *Mobula alfredi*, *M. birostris*, their symbionts, and other fishes in the Maldives. *PLOS ONE* 16:e0253704
- ✦ Notarbartolo di Sciara G (1987) A revisionary study of the genus *Mobula* Rafinesque, 1810 (Chondrichthyes: Mobulidae) with the description of a new species. *Zool J Linn Soc* 91:1–91
- ✦ Oliver SP, Hussey NE, Turner JR, Beckett AJ (2011) Oceanic sharks clean at coastal seamount. *PLOS ONE* 6:e14755
- ✦ O'Toole B (2002) Phylogeny of the species of the superfamily Echeneoidea (Perciformes: Carangoidei: Echeneidae, Rachycentridae, and Coryphaenidae), with an interpretation of echeneid hitchhiking behaviour. *Can J Zool* 80: 596–623
- ✦ Palacios MD, Stewart JD, Croll DA, Cronin MR and others (2023) Manta and devil ray aggregations: conservation challenges and developments in the field. *Front Mar Sci* 10:1148234
- ✦ Parenti P (2021) Checklist of fishes of the family Echeneidae. *Int J Zool Investig* 7:566–573
- ✦ R Core Team (2022) R: a language and environment for statistical computing. R Foundation for Statistical Computing, Vienna. <https://www.R-project.org/>
- ✦ Ritter EK (2002) Analysis of sharksucker, *Echeneis naucrates*, induced behavior patterns in the blacktip shark, *Carcharhinus limbatus*. *Environ Biol Fishes* 65:111–115
- ✦ Ritter EK, Brunnschweiler JM (2003) Do sharksuckers, *Echeneis naucrates*, induce jump behaviour in blacktip sharks, *Carcharhinus limbatus*? *Mar Freshwat Behav Physiol* 36: 111–113
- ✦ Sakamoto KQ, Sato K, Ishizuka M, Watanuki Y, Takahashi A, Daunt F, Wanless S (2009) Can ethograms be automatically generated using body acceleration data from free-ranging birds? *PLOS ONE* 4:e5379
- ✦ Sanches JG (1991) *Catálogo dos principais peixes marinhos da República de Guiné-Bissau*. Publicações Avulsas do INIP 16. Instituto Nacional de Investigação das Pescas, Lisboa
- ✦ Sequeira AMM, Thums M, Brooks K, Meekan MG (2016) Error and bias in size estimates of whale sharks: implica-

- tions for understanding demography. *R Soc Open Sci* 3: 150668
- ✦ Sheaves M, Mattone C, Barnett A, Abrantes K and others (2024) Whale sharks as oceanic nurseries for golden trevally. *Pac Conserv Biol* 30:PC23004
- Shortis M, Harvey E (1998) Design and calibration of an underwater stereo-video system for the monitoring of marine fauna populations. *Int Arch Photogramm Remote Sens* 32:792–799
- Shortis M, Harvey E, Abdo D (2009) A review of underwater stereo-image measurement for marine biology and ecology applications. *Oceanogr Mar Biol Annu Rev* 47: 257–292
- ✦ Silva JM Jr, Sazima I (2003) Whalesuckers and spinner dolphins bonded for weeks: Does host fidelity pay off? *Biota Neotrop* 3:1–5
- ✦ Silva JM Jr, Sazima I (2008) Whalesuckers on spinner dolphins: an underwater view. *Mar Biodivers Rec* 1:e22
- Silverman BW (1986) Density estimation for statistics and data analysis. Chapman & Hall, New York, NY
- ✦ Sobral A, Afonso P (2014) Occurrence of mobulids in the Azores, central North Atlantic. *J Mar Biol Assoc UK* 94: 1671–1675
- ✦ Solleliet-Ferreira S, Macena BCL, Laglbauer BJL, Sobral AF, Afonso P, Fontes J (2020) Sicklefin devilray and common remora prey jointly on baitfish. *Environ Biol Fishes* 103: 993–1000
- ✦ Stewart JD, Barroso A, Butler RH, Munns RJ (2018) Caught at the surface: myctophids make easy prey for dolphins and devil rays. *Ecology* 99:1894–1896
- ✦ Strasburg D (1962) Some aspects of the feeding behavior of *Remora remora*. *Pac Sci* 16:202–206
- ✦ Thorrold SR, Afonso P, Fontes J, Braun CD, Santos RS, Skomal GB, Berumen ML (2014) Extreme diving behaviour in devil rays links surface waters and the deep ocean. *Nat Commun* 5:4274
- Weihls D, Webb PW (1983) Optimization of locomotion. In: Webb PW, Weihls D (eds) *Fish biomechanics*. Praeger, New York, NY, p 339–371
- ✦ Weihls D, Fish FE, Nicasastro AJ (2007) Mechanics of remora removal by dolphin spinning. *Mar Mamm Sci* 23:707–714
- ✦ White WT, Corrigan S, Yang L, Henderson AC, Bazinet AL, Swofford DL, Naylor GJP (2018) Phylogeny of the manta and devilrays (Chondrichthyes: Mobulidae), with an updated taxonomic arrangement for the family. *Zool J Linn Soc* 182:50–75
- Whitehead PJP (1984) *Fishes of the north-eastern Atlantic and the Mediterranean*. UNESCO, Paris
- ✦ Williams EH Jr, Mignucci-Giannoni AA, Bunkley-Williams L, Bonde RK, Self-Sullivan C, Preen A, Cockcroft VG (2003) Echeneid–sirenian associations, with information on sharksucker diet. *J Fish Biol* 63:1176–1183
- ✦ Wingert N, Milmann L, Baumgarten M, Danilewicz D, Sazima I, Ott P (2021) Relationships between common bottlenose dolphins (*Tursiops truncatus*) and whalesuckers (*Remora australis*) at a remote archipelago in the equatorial Atlantic Ocean. *Aquat Mamm* 47:585–598
- ✦ Xu Y, Shi W, Arredondo-Galeana A, Mei L, Demirel YK (2021) Understanding of remora's 'hitchhiking' behaviour from a hydrodynamic point of view. *Sci Rep* 11:14837

Editorial responsibility: Franz Mueter,  
Juneau, Alaska, USA  
Reviewed by: C. P. Kenaley and 2 anonymous referees

Submitted: October 15, 2023  
Accepted: November 8, 2024  
Proofs received from author(s): January 13, 2025